Decentralized AC Optimal Power Flow for Integrated Transmission and Distribution Grids

Chenhui Lin, *Student Member, IEEE*, Wenchuan Wu, *Senior Member, IEEE*, and Mohammad Shahidehpour, *Fellow, IEEE*

***Abstract*—The coordinated solution of AC optimal power flow (ACOPF) in the integrated transmission and distribution grid utilizes controllable energy resources in distribution grids for introducing additional operational economy and security benefits of power grids. However, it is rather impractical to compute the ACOPF centrally considering the information privacy in the operation of transmission and distribution grids. Due to the large capacity of distributed generators integrated to distribution grids, existing decentralized methods may encounter numerical problems and fail to converge when nonlinear ACOPF models are applied. In this paper, we propose a decentralized method to solve the ACOPF for integrated transmission and distribution grids. The proposed ACOPF model is characterized through polar-coordinate equations and branch flow equations for transmission grids and distribution grids respectively. A distribution-cost-correction framework is developed for a fast-convergent solution which is based on approximated distribution cost functions. A rigorous proof is provided for convergence and numerical simulations are analyzed for standard IEEE systems which demonstrate the advantages of the coordinated approach in reducing generation dispatch costs and mitigating overvoltage problems. The paper validates through simulations that the accuracy, computational efficiency, and scalability of the proposed approach are superior to those of traditional methods.**

***Index Terms*—Integrated transmission and distribution grids, AC optimal power flow, decomposition methods, second-order cone relaxation.**

NOMENCLATURE

Sets

IB_T	Index set of buses of the transmission grid
IG_T	Index set of generators of the transmission grid
IG_{Ti}	Index set of generators connected to bus i of the transmission grid
IL_T	Index set of lines of the transmission grid
ID	Index set of distribution grids
IB_{D_k}	Index set of buses of distribution grid k
IG_{D_k}	Index set of generators of distribution grid k
$IG_{D_k i}$	Index set of generators connected to bus i of distribution grid k
IL_{D_k}	Index set of lines of distribution grid k.

Variables

P_{Tij}	Active power flow of line ij of the transmission grid
P_{Ti}^G	Active power output of generator i of the transmission grid
Q_{Tij}	Reactive power flow of line ij of the transmission grid
Q_{Ti}^G	Reactive power output of generator i of the transmission grid
θ_{Ti}	Voltage angle of bus i of the transmission grid
V_{Ti}	Voltage magnitude of bus i of the transmission grid
$l_{D_k ij}$	Square of current magnitude of line ij of distribution grid k
$P_{D_k ij}$	Active power flow of line ij of distribution grid k
$P_{D_k i}^G$	Active power output of generator i of distribution grid k
$Q_{D_k ij}$	Reactive power flow of line ij of distribution grid k
$Q_{D_k i}^G$	Reactive power output of generator i of distribution grid k
$v_{D_k i}$	Square of voltage magnitude of bus i of distribution grid k.

Parameters

a_{Ti}, b_{Ti}, c_{Ti}	Quadratic, linear, and constant terms in the quadratic generation cost function of generator i of the transmission grid
b_{Tij}^C	Line charging susceptance of line ij of the transmission grid
b_{Tij}^ε	Susceptance of line ij of the transmission grid
b_{Ti}^s	Shunt susceptance at bus i of the transmission grid
ϕ_{Tij}	Transformer phase shift angle of line ij of the transmission grid

Manuscript received May 1, 2019; revised October 4, 2019; accepted November 28, 2019. Date of publication December 3, 2019; date of current version April 21, 2020. This work was supported by the National Natural Science Foundation of China under Grant 51725703. Paper no. TSG-00621-2019. *(Corresponding author: Wenchuan Wu.)*

C. Lin and W. Wu are with the State Key Laboratory of Power Systems, Department of Electrical Engineering, Tsinghua University, Beijing 100084, China (e-mail: wuwench@tsinghua.edu.cn).

M. Shahidehpour is with the Robert W. Galvin Center for Electricity Innovation, Illinois Institute of Technology, Chicago, IL 60616 USA (e-mail: ms@iit.edu).

Color versions of one or more of the figures in this article are available online at http://ieeexplore.ieee.org.

Digital Object Identifier 10.1109/TSG.2019.2957142

g^{ε}_{Tij} Conductance of line ij of the transmission grid

g^{s}_{Ti} Shunt conductance at bus i of the transmission grid

i_{BTk} The index of the bus in the transmission grid connected with distribution grid k

i_{GTk} The index of the equivalent generator for distribution grid k in the transmission grid

P^{D}_{Ti} Active power load at bus i of the transmission grid

$\overline{P^{G}_{Ti}}, \underline{P^{G}_{Ti}}$ Upper/lower active power output bound of generator i of the transmission grid

Q^{D}_{Ti} Reactive power load at bus i of the transmission grid

$\overline{Q^{G}_{Ti}}, \underline{Q^{G}_{Ti}}$ Upper/lower reactive power output bound of generator i of the transmission grid

$\overline{S_{Tij}}$ Capacity of line ij of the transmission grid

τ_{Tij} Transformer tap ratio of line ij of the transmission grid

$\overline{V_{Ti}}, \underline{V_{Ti}}$ Upper/lower voltage magnitude bound of bus i of the transmission grid

$a_{D_ki}, b_{D_ki}, c_{D_ki}$ Quadratic, linear, and constant terms in the quadratic generation cost function of generator i of distribution grid k

i_{BDk} The index of the bus in distribution grid k connected with the transmission grid

i_{GDk} The index of the equivalent generator for the transmission grid in distribution grid k

$\overline{l_{D_kij}}$ Upper bound for the square of current magnitude of line ij of distribution grid k

$P^{D}_{D_ki}$ Active power load at bus i of distribution grid k

$\overline{P^{G}_{D_ki}}, \underline{P^{G}_{D_ki}}$ Upper/lower active power output bound of generator i of distribution grid k

$Q^{D}_{D_ki}$ Reactive power load at bus i of distribution grid k

$\overline{Q^{G}_{D_ki}}, \underline{Q^{G}_{D_ki}}$ Upper/lower reactive power output bound of generator i of distribution grid k

r_{D_kij} Resistance of line ij of distribution grid k

$\overline{v_{D_ki}}, \underline{v_{D_ki}}$ Upper/lower bound for the square of voltage magnitude of bus i of distribution grid k

x_{D_kij} Reactance of line ij of distribution grid k.

I. INTRODUCTION

A. Background

THE DEVELOPMENT of active distribution grids makes it possible for a large set of distributed generators (DGs) and renewable energy sources (RESs) to be integrated directly into the electricity grid [1]–[3]. However, an arising challenge is that the flexibility provided by distribution grids are insufficient for large integrations of variable resources. To increase the integration of allowable DG capacity, the coordination of transmission and distribution grids are considered indispensable. Conventionally, transmission and distribution grids are operated and optimized independently by their respective operators which could hinder the exploitation of flexible resources in two-level grids.

The coordinated economic dispatch of transmission and distribution grids (TD-ED) with RES could reduce the power generation and delivery costs through appropriately scheduled generation resources in the two grids. However, there are also significant drawbacks with respect to the TD-ED implementation. First, active and reactive power flows cannot be decoupled in active distribution grids and disregarding the reactive power supply in TD-ED could result in large errors. Second, DG integration in active distribution grids is critically restricted by bus voltage issues caused by reversed power flows. Large power injections into active distribution grids could result in overvoltage problems at corresponding buses. Consequently, TD-ED which only considers active power flows can only provide a rough power grid solution. Therefore, it is imperative to compute the coordinated AC optimal power flow (ACOPF) of transmission and distribution grids, in which both active and reactive power flows are determined.

However, it is impractical to combine transmission and distribution grid models and solve a single ACOPF centrally due to the confidentiality of system data and the provision of independent decisions rendered by individual operators at all levels. Thus, a coordinated and decentralized transmission and distribution ACOPF (TD-ACOPF) should be investigated for considering the RES role. However, TD-ACOPF model is nonlinear and nonconvex, which is hard to solve and even more difficult to be implemented in a decentralized manner. Most decomposition methods, such as Benders decomposition [4], require linear constraints for efficiency, which are generally inappropriate to the nonlinear TD-ACOPF model. Although dual decomposition methods can fit nonlinear models, there is no theoretical evidence supporting the convergence of dual decomposition methods in nonconvex ACOPF models. Therefore, it is quite necessary to look for a stable, robust, and scalable decentralized method to deal with a coordinated solution of the TD-ACOPF problem.

B. Related Literature

The coordinated solution of transmission and distribution grids has been investigated in recent studies and several decentralized algorithms have been reviewed in [5]. Article [6] proposes a heterogeneous decomposition method to deal with the coordinated TD-ED, and a multi-parametric programming method is proposed in [7]. In [8], an iteration framework is developed for enhancing the TD-ED solution with RES.

A number of decomposition methods have been proposed for decentralized operation problems. In particular, [9], [10] deal with nonlinear operation of the transmission and distribution coordination problem. The heterogeneous decomposition in [6] is extended to solve the ACOPF problem in [9]. Similar dual decomposition methods include the alternating direction method of multipliers (ADMM) [11], auxiliary problem principle (APP) [12], and optimality condition decomposition (OCD) [13]. In [10], the generalized

Benders decomposition method [14] is used to decompose the coordinated transmission and distribution reactive power optimization. However, its convergence rate is influenced by the nonlinear objective function in ACOPF.

C. Contributions

This paper aims to propose a decentralized method to the coordinated TD-ACOPF problem which provides an improved solution with guaranteed convergence compared with existing methods. A distribution-cost-correction framework is developed which can successfully handle the nonlinearity in ACOPF. The distribution-cost-correction framework uses the lower bound of each generation cost in active distribution grid to provide an iterative optimal solution for the coordinated transmission and distribution grids. In the distribution-cost-correction framework, the convergence in the iterative solution is managed by the lower bound gap. Consequently, we propose closer quadratically approximated functions for improving the convergence rates of the TD-ACOPF problem.

The novelty of the proposed method is that it provides more stable and efficient TD-ACOPF solutions compared with existing methods. Firstly, it deals with the nonconvex transmission grid ACOPF in the primal space instead of dual space, which makes the solution more stable. Secondly, unlike the generalized Benders decomposition, the proposed method transforms sub-problem infeasibility by relaxing boundary constraint and penalizing it into the objective, so numerical failures with respect to sub-problem infeasibility can be avoided. Thirdly, the proposed method uses a quadratically approximated function of the distribution cost to improve the coordination efficiency between transmission and distribution grids.

The remainder of this paper is arranged as follows. Detailed formulations of the TD-ACOPF problem are provided in Section II. Section III introduces the distribution-cost-correction framework and proposes lower bound functions and quadratically approximated functions of the distribution grid cost to implement this framework. Case studies are conducted in Section IV, which prove the validity of the proposed decentralized method and its performance compared with other methods. Conclusions are drawn in Section V.

II. Problem Formulation of TD-ACOPF

A. Objective Function

The TD-ACOPF problem minimizes the total generation cost in transmission and distribution grids. Each individual generation cost is expressed as a quadratic function of active power:

$$\min \sum_{i\in IG_T} a_{Ti}\left(P_{Ti}^G\right)^2 + b_{Ti}P_{Ti}^G + c_{Ti} + \sum_{k\in ID}\sum_{i\in IG_{D_k}} a_{D_ki}\left(P_{D_ki}^G\right)^2 + b_{D_ki}P_{D_ki}^G + c_{D_ki}. \quad (1)$$

B. Constraints

Constraints include those in transmission and distribution grids and the respective coupling constraints as presented next.

1) Transmission Grid Constraints: Transmission power flow equations are presented in polar coordinates with limits on generators' active and reactive power outputs, line flows, and bus voltage magnitudes:

$$P_{Tij} = \frac{1}{\tau_{Tij}^2} g_{Tij}^{\varepsilon} V_{Ti}^2 - \frac{1}{\tau_{Tij}} V_{Ti}V_{Tj}\Big[g_{Tij}^{\varepsilon}\cos\left(\theta_{Ti}-\theta_{Tj}-\phi_{Tij}\right) + b_{Tij}^{\varepsilon}\sin\left(\theta_{Ti}-\theta_{Tj}-\phi_{Tij}\right)\Big], \quad \forall ij \in IL_T \quad (2)$$

$$P_{Tji} = g_{Tij}^{\varepsilon} V_{Tj}^2 - \frac{1}{\tau_{Tij}} V_{Ti}V_{Tj}\Big[g_{Tij}^{\varepsilon}\cos\left(\theta_{Tj}-\theta_{Ti}+\phi_{Tij}\right) + b_{Tij}^{\varepsilon}\sin\left(\theta_{Tj}-\theta_{Ti}+\phi_{Tij}\right)\Big], \quad \forall ij \in IL_T \quad (3)$$

$$Q_{Tij} = -\frac{1}{\tau_{Tij}^2}\left(b_{Tij}^{\varepsilon} + \frac{b_{Tij}^C}{2}\right)V_{Ti}^2 - \frac{1}{\tau_{Tij}}V_{Ti}V_{Tj} \times \Big[g_{Tij}^{\varepsilon}\sin\left(\theta_{Ti}-\theta_{Tj}-\phi_{Tij}\right) - b_{Tij}^{\varepsilon}\cos\left(\theta_{Ti}-\theta_{Tj}-\phi_{Tij}\right)\Big], \quad \forall ij \in IL_T \quad (4)$$

$$Q_{Tji} = -\left(b_{Tij}^{\varepsilon} + \frac{b_{Tij}^C}{2}\right)V_{Tj}^2 - \frac{1}{\tau_{Tij}}V_{Ti}V_{Tj} \times \Big[g_{Tij}^{\varepsilon}\sin\left(\theta_{Tj}-\theta_{Ti}+\phi_{Tij}\right) - b_{Tij}^{\varepsilon}\cos\left(\theta_{Tj}-\theta_{Ti}+\phi_{Tij}\right)\Big], \quad \forall ij \in IL_T \quad (5)$$

$$\sum_{j\in IG_{Ti}} P_{Tj}^G - \sum_{j:ji\in IL_T} P_{Tij} - \sum_{j:ij\in IL_T} P_{Tij} - P_{Ti}^D - V_{Ti}^2 g_{Ti}^s = 0, \quad \forall i \in IB_T \quad (6)$$

$$\sum_{j\in IG_{Ti}} Q_{Tj}^G - \sum_{j:ji\in IL_T} Q_{Tij} - \sum_{j:ij\in IL_T} Q_{Tij} - Q_{Ti}^D + V_{Ti}^2 b_{Ti}^s = 0, \quad \forall i \in IB_T \quad (7)$$

$$\underline{V_{Ti}} \le V_{Ti} \le \overline{V_{Ti}}, \quad \forall i \in IB_T \quad (8)$$

$$\underline{P_{Ti}^G} \le P_{Ti}^G \le \overline{P_{Ti}^G},\ \underline{Q_{Ti}^G} \le Q_{Ti}^G \le \overline{Q_{Ti}^G}, \quad \forall i \in IG_T \quad (9)$$

$$P_{Tij}^2 + Q_{Tij}^2 \le \overline{S_{Tij}}^2,\ P_{Tji}^2 + Q_{Tji}^2 \le \overline{S_{Tij}}^2, \quad \forall ij \in IL_T \quad (10)$$

Equations (2)-(5) compute active and reactive branch flows; equations (6)-(7) are power balance constraints of each bus; equation (8) denotes the upper and lower bus voltage magnitude limits; equation (9) is the power output limit of each generator; equation (10) is the transmission capacity constraint.

2) Distribution Grid Constraints: For radial distribution grids, a branch flow model [15]–[17] is used which does not include voltage angle variables. This model can fully exploit good features of radial grids, and can be further relaxed to a convex form, which will benefit our proposed solution.

$$P_{D_kij}^2 + Q_{D_kij}^2 = v_{D_ki} l_{D_kij}, \quad \forall ij \in IL_{D_k}, \ \forall k \in ID \quad (11)$$

$$\sum_{j\in IG_{D_ki}} P_{D_kj}^G + \sum_{j:ji\in IL_{D_k}} \left(P_{D_kji} - l_{D_kji} r_{D_kji}\right) = \sum_{j:ij\in IL_{D_k}} P_{D_kij} + P_{D_ki}^D, \quad \forall i \in IB_{D_k}, \ \forall k \in ID \quad (12)$$

$$\sum_{j\in IG_{D_k i}} Q_{D_k j}^G + \sum_{j:ji\in IL_{D_k}} \left(Q_{D_k ji} - l_{D_k ji} x_{D_k ji}\right) = \sum_{j:ij\in IL_{D_k}} Q_{D_k ij} + Q_{D_k i}^D,\ \forall i \in IB_{D_k},\ \forall k \in ID \quad (13)$$

$$v_{D_k j} = v_{D_k i} - 2\left(r_{D_k ij} P_{D_k ij} + x_{D_k ij} Q_{D_k ij}\right) + \left(r_{D_k ij}^2 + x_{D_k ij}^2\right) l_{D_k ij},\ \forall ij \in IL_{D_k},\ \forall k \in ID \quad (14)$$

$$\underline{v_{D_k i}} \le v_{D_k i} \le \overline{v_{D_k i}},\ \forall i \in IB_{D_k},\ \forall k \in ID \quad (15)$$

$$\underline{P_{D_k i}^G} \le P_{D_k i}^G \le \overline{P_{D_k i}^G},\ \underline{Q_{D_k i}^G} \le Q_{D_k i}^G \le \overline{Q_{D_k i}^G},\ \forall i \in IG_{D_k},\ \forall k \in ID \quad (16)$$

$$l_{D_k ij} \le \overline{l_{D_k ij}},\ \forall ij \in IL_{D_k},\ \forall k \in ID \quad (17)$$

Here, $l_{D_k ij}$ and $v_{D_k i}$ are the square of current and voltage magnitudes. By using the squares of voltage and current magnitudes, equations (12)-(14) can be linearized and convexified.

Among all distribution grid constraints, equation (11) computes the square of branch flow magnitudes; equations (12)-(13) are bus active and reactive power balance constraints; equation (14) describes the voltage magnitude square difference of the two terminals of each branch, whose derivation can be achieved from [16]; equations (15)-(17) are operation limits of bus voltage magnitudes, generator power outputs, and line current magnitudes respectively.

A nearly exact second-order cone relaxation is used to convexify this model [16]–[18]. Constraint (11) is relaxed into a rotated second-order cone:

$$P_{D_k ij}^2 + Q_{D_k ij}^2 \le v_{D_k i} l_{D_k ij},\ \forall ij \in IL_{D_k},\ \forall k \in ID \quad (18)$$

Consequently, distribution constraints are all convex, consisting of linear constraints (12)-(17) and second-order cone constraints (18). The convexity of the distribution grid model will be used in the following discussion.

3) Coupling Constraints: Coupling constraints for transmission and distribution grids represent consistencies in boundary power and voltage magnitudes. The transferred power between the transmission grid and the distribution grid is considered as an equivalent generator of each distribution grid and a negative equivalent generator of the transmission grid. The coupling constraints are:

$$P_{Ti_{GTk}}^G = -P_{D_k i_{GDk}}^G,\ \forall k \in ID \quad (19)$$

$$Q_{Ti_{GTk}}^G = -Q_{D_k i_{GDk}}^G,\ \forall k \in ID \quad (20)$$

$$V_{Ti_{BTk}}^2 = v_{D_k i_{BDk}},\ \forall k \in ID. \quad (21)$$

C. Reformulation of TD-ACOPF

The TD-ACOPF problem, which minimizes (1) with constraints (2)-(10) and (12)-(21), is represented in a compact form in order to better introduce the decentralized solution.

$$\min_{\mathbf{x}_T, \mathbf{x}_{D_k}} \quad C_T(\mathbf{x}_T) + \sum_{k\in ID} C_{D_k}\left(\mathbf{x}_{D_k}\right) \quad (22a)$$

$$\text{subject to} \quad \mathbf{F}_T(\mathbf{x}_T) \le \mathbf{0} \quad (22b)$$

$$\mathbf{F}_{D_k}\left(\mathbf{x}_{D_k}\right) \le \mathbf{0},\ \forall k \in ID \quad (22c)$$

$$\mathbf{G}_k(\mathbf{x}_T) = \mathbf{H}_k \mathbf{x}_{D_k},\ \forall k \in ID \quad (22d)$$

In problem (22), vector $\mathbf{x}_T$ denotes transmission grid variables, including P_{Tij}, Q_{Tij}, P_{Ti}^G, Q_{Ti}^G, V_{Ti}, and θ_{Ti}. Vector $\mathbf{x}_{D_k}$ denotes variables of distribution grid k, including $P_{D_k ij}$, $Q_{D_k ij}$, $P_{D_k i}^G$, $Q_{D_k i}^G$, $v_{D_k i}$, and $l_{D_k ij}$. Equation (22b) includes all transmission grid constraints (2)-(10), and equation (22c) includes all distribution grid constraints (12)-(18). Equation (22d) is the compact form of boundary constraints (19)-(21), where $\mathbf{G}_k(\mathbf{x}_T)$ is the vector $[P_{Ti_{GTk}}^G \quad Q_{Ti_{GTk}}^G \quad V_{Ti_{BTk}}^2]^T$, and $\mathbf{H}_k \mathbf{x}_{D_k}$ is the vector $[-P_{D_k i_{GDk}}^G \quad -Q_{D_k i_{GDk}}^G \quad v_{D_k i_{BDk}}]^T$.

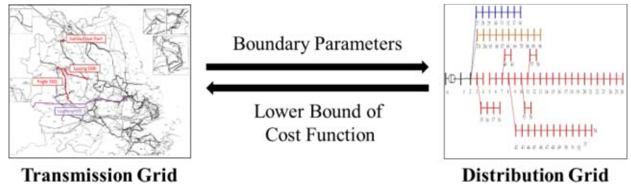

Fig. 1. Distribution-cost-correction framework.

III. Decentralized Solution Method

A. General Framework

The proposed decentralized method for TD-ACOPF is based on a distribution-cost-correction framework, which is depicted in Fig. 1.

In the distribution-cost-correction framework, the transmission grid performs its ACOPF initially by:

$$\min_{\mathbf{x}_T} \quad C_T(\mathbf{x}_T) \quad (23a)$$

$$\text{subject to} \quad \mathbf{F}_T(\mathbf{x}_T) \le \mathbf{0} \quad (23b)$$

The optimal solution of (23) is denoted by $\mathbf{x}_T^{(0)}$, of which the boundary parameter $\mathbf{G}_k(\mathbf{x}_T^{(0)})$ is transferred to distribution grid k for solving a local ACOPF stated as:

$$\min_{\mathbf{x}_{D_k}} \quad C_{D_k}\left(\mathbf{x}_{D_k}\right) \quad (24a)$$

$$\text{subject to} \quad \mathbf{F}_{D_k}\left(\mathbf{x}_{D_k}\right) \le \mathbf{0} \quad (24b)$$

$$\mathbf{H}_k \mathbf{x}_{D_k} = \mathbf{G}_k\left(\mathbf{x}_T^{(0)}\right) \quad (24c)$$

Problem (24) is actually an ACOPF of distribution grid k with boundary variables $P_{D_k i_{GDk}}^G$, $Q_{D_k i_{GDk}}^G$, and $v_{D_k i_{BDk}}$ fixed by the transmission grid solution.

A function $L_{D_k}(\mathbf{x}_T)$ is generated, which satisfies:

$$L_{D_k}(\mathbf{x}_T) \le C_{D_k}\left(\mathbf{x}_{D_k}\right) \quad (25)$$

for any $\mathbf{x}_T$, $\mathbf{x}_{D_k}$ satisfying (24b) and $\mathbf{H}_k \mathbf{x}_{D_k} = \mathbf{G}_k(\mathbf{x}_T)$. In other words, $L_{D_k}(\mathbf{x}_T)$ is a lower bound of distribution cost with respect to $\mathbf{x}_T$. Details for the deduction of $L_{D_k}(\mathbf{x}_T)$ will be introduced in the following sub-section.

The lower bounds of each distribution cost are considered in the transmission grid ACOPF:

$$\min_{\mathbf{x}_T, \alpha_k} \quad C_T(\mathbf{x}_T) + \sum_{k\in ID} \alpha_k \quad (26a)$$

$$\text{subject to} \quad \mathbf{F}_T(\mathbf{x}_T) \le 0 \quad (26b)$$

$$\alpha_k \ge L_{D_k}(\mathbf{x}_T),\ \forall k \in ID \quad (26c)$$

In problem (26), variable α_k denotes the cost of distribution grid k, which is constrained by (26c) as its lower bound.

Problem (26) provides an updated solution of $\mathbf{x}_T$, which is used in each distribution grid for updating $L_{D_k}(\mathbf{x}_T)$, thus the iteration between transmission and distribution grids will continue. If multiple lower bounds $L_{D_k}(\mathbf{x}_T)$ of distribution cost are generated and considered in (26c), the problem in (26) will converge to the optimal solution of the global problem (22) given that the combinations of different lower bounds $L_{D_k}(\mathbf{x}_T)$ of distribution cost could approach the actual distribution cost.

According to the framework provided by distribution-cost-correction, the transmission grid provides boundary parameters, while each distribution grid generates lower bounds of its optimal generation cost. In each iteration, a lower bound function for distribution cost will be generated to correct α_k in (26).

B. Simple Implementation of Distribution-Cost-Correction

Based on the above framework, a simple implementation is given below. Before giving the detailed full procedures, the lower bound function $L_{D_k}(\mathbf{x}_T)$ should be computed. Besides, inappropriate boundary parameters might cause infeasible distribution gird ACOPF. This also needs to be solved.

1) Derivation of Lower Bound of Distribution Cost: The distribution grid ACOPF is rewritten as:

$$\min_{\mathbf{x}_{D_k}} \quad C_{D_k}\left(\mathbf{x}_{D_k}\right) \tag{27a}$$

$$\text{subject to} \quad \mathbf{F}_{D_k}\left(\mathbf{x}_{D_k}\right) \leq \mathbf{0} \tag{27b}$$

$$\mathbf{H}_k \mathbf{x}_{D_k} = \mathbf{g}_k \tag{27c}$$

where $\mathbf{g}_k$ is the value of $\mathbf{G}_k(\mathbf{x}_T)$.

If $\mathbf{g}_k$ varies in (27c), the optimal objective of (27) varies correspondingly, which forms a function denoted by $C_{D_k-T}(\mathbf{g}_k)$. The relaxation of (18) provides a convex $C_{D_k-T}(\mathbf{g}_k)$ so that its tangent plane is one of its lower bounds.

Assume the boundary variables provided by transmission grid is $\hat{\mathbf{g}}_k$. The corresponding optimal solution of (27) is denoted by $\hat{\mathbf{x}}_{D_k}$. The tangent plane of $C_{D_k-T}(\mathbf{g}_k)$ at $\hat{\mathbf{g}}_k$ is:

$$L_{D_k}\left(\mathbf{g}_k\right) = C_{D_k}\left(\hat{\mathbf{x}}_{D_k}\right) - \hat{\boldsymbol{\lambda}}_k^T\left(\mathbf{g}_k - \hat{\mathbf{g}}_k\right) \tag{28}$$

where $\hat{\boldsymbol{\lambda}}_k$ is the vector of dual variables corresponding to (27c).

2) Distribution Grid Infeasibility: The distribution grid ACOPF (27) could be infeasible if boundary variables are poorly passed from the transmission grid. To avoid infeasibility, the distribution grid ACOPF is modified by relaxing boundary constraints and instead adding a penalty term for violating boundary coupling constraints. The modified distribution grid ACOPF is:

$$\min_{\mathbf{x}_{D_k},\boldsymbol{\beta}_k,\boldsymbol{\gamma}_k} \quad C_{D_k}\left(\mathbf{x}_{D_k}\right) + \mathbf{k}_{PEN}^T\left(\boldsymbol{\beta}_k + \boldsymbol{\gamma}_k\right) \tag{29a}$$

$$\text{subject to} \quad \mathbf{F}_{D_k}\left(\mathbf{x}_{D_k}\right) \leq \mathbf{0} \tag{29b}$$

$$\mathbf{H}_k \mathbf{x}_{D_k} + \boldsymbol{\beta}_k - \boldsymbol{\gamma}_k = \hat{\mathbf{g}}_k \tag{29c}$$

$$\boldsymbol{\beta}_k \geq 0, \boldsymbol{\gamma}_k \geq 0 \tag{29d}$$

The penalty coefficient vector $\mathbf{k}_{PEN}$ is set large enough so that the distribution grid cost will be very large when the distribution grid is infeasible. This parameter should be sufficiently greater than the marginal generation cost of the corresponding distribution grid. Setting this parameter very large is theoretically good, but this will also cause numerical problems in practice.

If the distribution grid ACOPF (27) is feasible, $\boldsymbol{\beta}_k$ and $\boldsymbol{\gamma}_k$ will be 0 due to their large coefficients in the objective function, in which case (27) and (29) are equivalent.

The lower bound (28) is also substituted to:

$$L_{D_k}\left(\mathbf{g}_k\right) = C_{D_k}\left(\hat{\mathbf{x}}_{D_k}\right) + \mathbf{k}_{PEN}^T\left(\hat{\boldsymbol{\beta}}_k + \hat{\boldsymbol{\gamma}}_k\right) - \hat{\boldsymbol{\lambda}}_k^T\left(\mathbf{g}_k - \hat{\mathbf{g}}_k\right) \tag{30}$$

where $\hat{\boldsymbol{\beta}}_k$ and $\hat{\boldsymbol{\gamma}}_k$ are optimal solutions of $\boldsymbol{\beta}_k$ and $\boldsymbol{\gamma}_k$ at $\hat{\mathbf{g}}_k$, $\hat{\boldsymbol{\lambda}}_k$ is the vector of dual variables corresponding to (29c).

If infeasibility occurs in the distribution grid problem, $\hat{\boldsymbol{\lambda}}_k$ will be very large, which will force boundary parameters $\mathbf{g}_k$ to move towards feasible directions in the following iteration.

Different from the proposed method to deal with distribution grid infeasibility, other methods such as the generalized Benders decomposition generate feasibility cuts which will be considered as additional constraints in the transmission grid. However, feasibility cuts will lead parameters $\mathbf{g}_k$ to be right at the boundary between distribution problem feasibility and infeasibility, which may make the updated model ill-conditioned. The proposed method avoids that disadvantage by making the distribution problem always feasible.

3) Iteration Procedure: Detailed iteration procedures of the simple implementation are summarized as below.

Step 1 (Transmission Grid): Initialize iteration number m as 0. The transmission grid ACOPF is solved through (23) with an optimal solution denoted by $\mathbf{x}_T^{(m)}$. Let $\mathbf{g}_k^{(m)}$ be $\mathbf{G}_k(\mathbf{x}_T^{(m)})$, which is the vector of parameters provided to distribution grid k.

Step 2 (Distribution Grid): Increase m by 1. Each distribution grid solves a modified ACOPF (29) using boundary parameters $\mathbf{g}_k^{(m-1)}$ which replaces $\hat{\mathbf{g}}_k$ in (29c).

The optimal solution of (29) is denoted as $\mathbf{x}_{D_k}^{(m)}$, $\boldsymbol{\beta}_k^{(m)}$, and $\boldsymbol{\gamma}_k^{(m)}$; the vector of dual variables corresponding to (29c) is denoted as $\boldsymbol{\lambda}_k^{(m)}$. Then the lower bound function of $\mathbf{x}_T$ is stated as:

$$L_{D_k}^{(m)}\left(\mathbf{g}_k\right) = C_{D_k}\left(\mathbf{x}_{D_k}^{(m)}\right) + \mathbf{k}_{PEN}^T\left(\boldsymbol{\beta}_k^{(m)} + \boldsymbol{\gamma}_k^{(m)}\right) - \left(\boldsymbol{\lambda}_k^{(m)}\right)^T\left(\mathbf{g}_k - \mathbf{g}_k^{(m-1)}\right). \tag{31}$$

Step 3 (Transmission Grid): After collecting lower bound functions from each distribution grid, the transmission grid optimizes considering distribution costs:

$$\min_{\mathbf{x}_T,\alpha_k} \quad C_T(\mathbf{x}_T) + \sum_{k\in ID} \alpha_k \tag{32a}$$

$$\text{subject to} \quad \mathbf{F}_T(\mathbf{x}_T) \leq 0 \tag{32b}$$

$$\alpha_k \geq L_{D_k}^{(l)}(\mathbf{G}_k(\mathbf{x}_T)), \ \forall l = 0, 1, \ldots, m, \ \forall k \in ID \tag{32c}$$

The optimal solution of (32) is denoted as $\mathbf{x}_T^{(m)}$. Accordingly, the optimal objective value of (32) is a lower bound of the optimal cost of the coordinated TD-ACOPF problem, which is denoted by $LB^{(m)}$. Besides, its upper bound can be computed by:

$$UB^{(m)} = C_T\left(\mathbf{x}_T^{(m-1)}\right) + \sum_{k\in ID} C_{D_k}\left(\mathbf{x}_{D_k}^{(m)}\right) + \mathbf{k}_{PEN}^T\left(\boldsymbol{\beta}_k^{(m)} + \boldsymbol{\gamma}_k^{(m)}\right) \tag{33}$$

As iteration number m increases, both $LB^{(m)}$ and $UB^{(m)}$ will converge to the optimal cost of the coordinated TD-ACOPF problem in which the convergence criterion is stated as:

$$UB^{(m)} - LB^{(m)} < \varepsilon \tag{34}$$

where ε is a small positive threshold. If (34) holds, $\mathbf{x}_T^{(m)}$ and $\mathbf{x}_{D_k}^{(m)}$ are the optimal solutions; otherwise, go back to step 2 for another iteration.

C. Discussion: Convergence Improvement

Although the procedure introduced in Section III-B can successfully solve the TD-ACOPF in a decentralized manner, its convergence speed might be slow. In the above implementation, the lower bound function $L_{D_k}^{(m)}(\mathbf{g}_k)$ in each distribution grid is a tangent plane of the real distribution cost $C_{D_k-T}(\mathbf{g}_k)$. Since the actual distribution cost $C_{D_k-T}(\mathbf{g}_k)$ is a nonlinear convex function, it may require a large number of tangent planes to approximate the actual distribution cost, which could lead to many iterations.

In this section, we find a quadratically approximated function of $C_{D_k-T}(\mathbf{g}_k)$, denoted as $Q_{D_k}^{(m)}(\mathbf{g}_k)$, such that

$$L_{D_k}^{(m)}(\mathbf{g}_k) \le C_{D_k-T}(\mathbf{g}_k) \approx Q_{D_k}^{(m)}(\mathbf{g}_k) \tag{35}$$

The distribution grid ACOPF is rewritten into the following form based on its characteristics:

$$\min_{\mathbf{x}_{D_k}^{ext}} \quad \frac{1}{2}\left(\mathbf{x}_{D_k}^{ext}\right)^T \mathbf{Q}_k^{ext}\mathbf{x}_{D_k}^{ext} + \left(\mathbf{c}_k^{ext}\right)^T \mathbf{x}_{D_k}^{ext} \tag{36a}$$

$$\text{subject to} \quad \mathbf{A}_k^{eq}\mathbf{x}_{D_k}^{ext} = \mathbf{b}_k^{eq} + \mathbf{E}_k\hat{\mathbf{g}}_k \tag{36b}$$

$$\mathbf{A}_k^{ineq}\mathbf{x}_{D_k}^{ext} \le \mathbf{b}_k^{ineq} \tag{36c}$$

$$\frac{1}{2}\left(\mathbf{x}_{D_k}^{ext}\right)^T \mathbf{Q}_k^{ci}\mathbf{x}_{D_k}^{ext} \le 0, \ \forall i \in I_k^{SOC} \tag{36d}$$

where $\mathbf{x}_{D_k}^{ext}$ is a generalized vector of distribution grid variables which includes $\mathbf{x}_{D_k}$, $\boldsymbol{\beta}_k$, and $\boldsymbol{\gamma}_k$; $\mathbf{Q}_k^{ext}$ and $\mathbf{c}_k^{ext}$ are quadratic and linear parameters of the objective function (29a); constraints (36b) and (36c) are equality and inequality constraints, respectively, among (12)-(17); I_k^{SOC} is the index set of second-order cone constraints; $\mathbf{Q}_k^{ci}$ is the quadratic parameter for second-order cone constraint i.

The optimal solution of (36) is denoted as $\hat{\mathbf{x}}_{D_k}^{ext}$, and dual variables of (36b)-(36d) are $\hat{\boldsymbol{\lambda}}_k^{eq}$, $\hat{\boldsymbol{\lambda}}_k^{ineq}$, and $\hat{\boldsymbol{\lambda}}_k^{qci}$.

The partial derivative of the Lagrange Function with respect to $\mathbf{x}_{D_k}^{ext}$ yields:

$$\mathbf{Q}_k^{ext}\hat{\mathbf{x}}_{D_k}^{ext} + \mathbf{c}_k^{ext} + \left(\mathbf{A}_k^{eq}\right)^T\hat{\boldsymbol{\lambda}}_k^{eq} + \left(\mathbf{A}_k^{ineq}\right)^T\hat{\boldsymbol{\lambda}}_k^{ineq} + \sum_{i\in I_k^{SOC}} \hat{\boldsymbol{\lambda}}_k^{qci}\mathbf{Q}_k^{ci}\hat{\mathbf{x}}_{D_k}^{ext} = 0 \tag{37}$$

The complementary slackness of (36c) and (36d) gives:

$$diag\left(\hat{\boldsymbol{\lambda}}_k^{ineq}\right) * \left(\mathbf{A}_k^{ineq}\hat{\mathbf{x}}_{D_k}^{ext} - \mathbf{b}_k^{ineq}\right) = 0 \tag{38}$$

$$\frac{1}{2}\hat{\boldsymbol{\lambda}}_k^{qci}\left(\hat{\mathbf{x}}_{D_k}^{ext}\right)^T \mathbf{Q}_k^{ci}\hat{\mathbf{x}}_{D_k}^{ext} = 0, \ \forall i \in I_k^{SOC} \tag{39}$$

We assume a small variation of boundary parameters from $\hat{\mathbf{g}}_k$ to $\hat{\mathbf{g}}_k + \mathrm{d}\mathbf{g}_k$. The optimal solutions of primal and dual variables at $\hat{\mathbf{g}}_k + \mathrm{d}\mathbf{g}_k$ are denoted as $\hat{\mathbf{x}}_{D_k}^{ext} + \mathrm{d}\mathbf{x}_{D_k}^{ext}$, $\hat{\boldsymbol{\lambda}}_k^{eq} + \mathrm{d}\boldsymbol{\lambda}_k^{eq}$, $\hat{\boldsymbol{\lambda}}_k^{ineq} + \mathrm{d}\boldsymbol{\lambda}_k^{ineq}$, and $\hat{\boldsymbol{\lambda}}_k^{qci} + \mathrm{d}\boldsymbol{\lambda}_k^{qci}$. Insert these new solutions into (36b) and (37)-(39), and compute the differences between these equalities while disregarding second-order terms of variations:

$$\mathbf{A}_k^{eq} * \mathrm{d}\mathbf{x}_{D_k}^{ext} - \mathbf{E}_k * \mathrm{d}\hat{\mathbf{g}}_k = 0 \tag{40}$$

$$\left(\mathbf{Q}_k^{ext} + \sum_{i\in I_k^{SOC}} \hat{\lambda}_k^{qci}\mathbf{Q}_k^{ci}\right) * \mathrm{d}\mathbf{x}_{D_k}^{ext} + \left(\mathbf{A}_k^{eq}\right)^T \mathrm{d}\boldsymbol{\lambda}_k^{eq} + \left(\mathbf{A}_k^{ineq}\right)^T \mathrm{d}\boldsymbol{\lambda}_k^{ineq} + \sum_{i\in I_k^{SOC}} \mathbf{Q}_k^{ci}\hat{\mathbf{x}}_{D_k}^{ext} * \mathrm{d}\lambda_k^{qci} = 0 \tag{41}$$

$$diag\left(\mathbf{A}_k^{ineq}\hat{\mathbf{x}}_{D_k}^{ext} - \mathbf{b}_k^{ineq}\right) * \mathrm{d}\boldsymbol{\lambda}_k^{ineq} + diag\left(\hat{\boldsymbol{\lambda}}_k^{ineq}\right) * \mathbf{A}_k^{ineq} * \mathrm{d}\mathbf{x}_{D_k}^{ext} = 0 \tag{42}$$

$$\frac{1}{2}\left(\hat{\mathbf{x}}_{D_k}^{ext}\right)^T \mathbf{Q}_k^{ci}\left(\hat{\mathbf{x}}_{D_k}^{ext}\right) * \mathrm{d}\hat{\lambda}_k^{qci} + \hat{\lambda}_k^{qci}\left(\hat{\mathbf{x}}_{D_k}^{ext}\right)^T \mathbf{Q}_k^{ci} * \mathrm{d}\mathbf{x}_{D_k}^{ext} = 0, \quad \forall i \in I_k^{SOC} \tag{43}$$

Variations $\mathrm{d}\mathbf{x}_{D_k}^{ext}$, $\mathrm{d}\boldsymbol{\lambda}_k^{eq}$, $\mathrm{d}\boldsymbol{\lambda}_k^{ineq}$, and $\mathrm{d}\hat{\lambda}_k^{qci}$ can be solved using linear equations (40)-(43). We use $\hat{\mathbf{M}}_k$ to express the linear coefficient matrix linking $\mathrm{d}\mathbf{x}_{D_k}^{ext}$ and $\mathrm{d}\mathbf{g}_k$ as:

$$\mathrm{d}\mathbf{x}_{D_k}^{ext} = \hat{\mathbf{M}}_k\mathrm{d}\mathbf{g}_k \tag{44}$$

The quadratically approximated function $Q_{D_k}^{(m)}(\mathbf{g}_k)$ is:

$$Q_{D_k}^{(m)}(\mathbf{g}_k) = \frac{1}{2}\left[\hat{\mathbf{x}}_{D_k}^{ext} + \hat{\mathbf{M}}_k(\mathbf{g}_k - \hat{\mathbf{g}}_k)\right]^T \mathbf{Q}_k^{ext} \times \left[\hat{\mathbf{x}}_{D_k}^{ext} + \hat{\mathbf{M}}_k(\mathbf{g}_k - \hat{\mathbf{g}}_k)\right] + \left(\mathbf{c}_k^{ext}\right)^T\left[\hat{\mathbf{x}}_{D_k}^{ext} + \hat{\mathbf{M}}_k(\mathbf{g}_k - \hat{\mathbf{g}}_k)\right] \tag{45}$$

Note that since second-order terms are neglected in (41)-(43), the quadratically approximated function $Q_{D_k}^{(m)}(\mathbf{g}_k)$ can only be considered valid within the neighborhood of $\hat{\mathbf{g}}_k$. Thus, the quadratically approximated functions $Q_{D_k}^{(m)}(\mathbf{g}_k)$ generated in previous iterations should not be kept in the ACOPF of the transmission grid, which is different from the way we handle $L_{D_k}^{(m)}(\mathbf{g}_k)$.

D. Implementation With Improved Convergence

With the quadratically approximated function $Q_{D_k}^{(m)}(\mathbf{g}_k)$, we state the steps for the proposed decentralized approach with an improved convergence as follows. The proof of theoretical convergence for this method is discussed in the Appendix.

Step 1 (Transmission Grid): Initialize the iteration number m as 0. The transmission grid applies ACOPF using (23), with an optimal solution denoted by $\mathbf{x}_T^{(m)}$. Let $\mathbf{g}_k^{(m)}$ be $\mathbf{G}_k(\mathbf{x}_T^{(m)})$, which is the vector of parameters provided to distribution grid k.

Step 2 (Distribution Grid): Increase m by 1. Each distribution grid solves a modified ACOPF (29) by setting $\hat{\mathbf{g}}_k$ in (29c) as $\mathbf{g}_k^{(m-1)}$. Then the tangent plane as the lower bound function $L_{D_k}^{(m)}(\mathbf{g}_k)$ is generated by (31). The quadratically approximated function $Q_{D_k}^{(m)}(\mathbf{g}_k)$ is computed by (45).

Step 3 (Transmission Grid): The transmission grid optimizes its solution considering distribution costs using lower bound

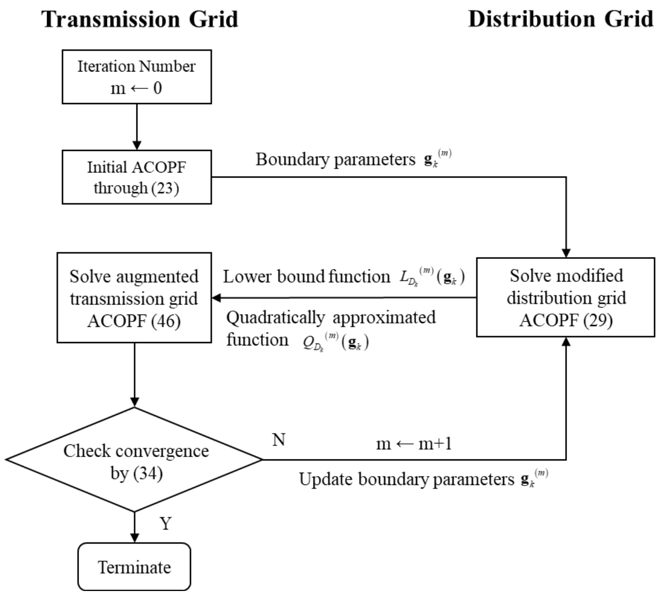

Fig. 2. Flow chart of the proposed method.

functions and quadratically approximated functions provided by each distribution grid:

$$\min_{\mathbf{x}_T,\alpha_k} \quad C_T(\mathbf{x}_T) + \sum_{k\in ID} \alpha_k \tag{46a}$$

$$\text{subject to} \quad \mathbf{F}_T(\mathbf{x}_T) \le 0 \tag{46b}$$

$$\alpha_k \ge L_{D_k}^{(l)}(\mathbf{G}_k(\mathbf{x}_T)), \ \forall l = 0, 1, \ldots, m, \ \forall k \in ID \tag{46c}$$

$$\alpha_k \ge Q_{D_k}^{(m)}(\mathbf{G}_k(\mathbf{x}_T)), \ \forall k \in ID \tag{46d}$$

The optimal solution of (46) is denoted as $\mathbf{x}_T^{(m)}$. The lower bound $LB^{(m)}$ is computed through (46a)-(46c) not considering (46d). The upper bound $UB^{(m)}$ is computed by (33). Check the convergence by (34). If (34) holds, $\mathbf{x}_T^{(m)}$ and $\mathbf{x}_{D_k}^{(m)}$ are the optimal solution; otherwise, go back to step 2 for another iteration.

E. Implementation Analysis

An overview of the proposed decentralized solution method can be shown in Fig. 2.

During the implementation, each distribution level control center computes a lower bound function and a quadratically approximated function of its optimal generation cost, with boundary variables fixed by the transmission grid. The transmission level control center performs an overall optimization of its generators and boundary coupled variables with all distribution grids, considering generation cost functions (lower bound and quadratically approximated) of distribution grids.

The information flow between transmission and distribution level control centers are summarized as follows: the transmission level control center passes boundary variables (active power, reactive power, voltage magnitude) to each distribution level control center; each distribution level control center passes lower bound functions and quadratically approximated functions of its optimal generation cost to the transmission level control center.

The share of boundary variables from the transmission grid to each distribution grid is required by any existing operation manners, otherwise there would be boundary mismatches. Therefore, boundary values should not be considered as a violation of privacies. The lower bound functions and quadratically approximated functions are both related to distribution generation costs, which are usually not related to security concerns. Even if the generation cost is considered as a private information that a distribution grid has concerns in sharing it, the distribution grid could add a constant bias to the two functions. Therefore, actual generation costs will not be exposed to the transmission grid. As long as the constant bias remain unchanged during iterations, the solution process will not be affected. As a consequence, there will be no security concerns with respect to information privacy in our proposed method.

IV. Case Studies

A. Numerical Simulation Settings

Two tests were generated based on the standard IEEE test systems. In System #1, a 14-bus transmission grid connects three 69-bus distribution grids at buses 10, 11, and 12. System #2 is larger, representing a 118-bus transmission grid connected to thirteen 69-bus distribution grids at buses 2, 7, 20, 28, 43, 44, 48, 50, 51, 52, 83, 97, and 117. We have added generators in the 69-bus distribution grid at buses 10, 20, 30, 40, and 50, to represent active distribution grids [19].

The numerical simulations are conducted on a laptop with an Intel i7-8550u CPU and 8GB RAM through MATLAB scripts. The IPOPT solver [20] is used for optimizations. The AC optimal power flow function provided in MATPOWER [21] is used as a benchmark to verify that our proposed solution provides correct ACOPF results. The convergence tolerance ε in (34) is set as 10^{-3}. The penalty coefficient vector $\mathbf{k}_{PEN}$ in (29a) is set as 100.

B. Effects of Coordination in ACOPF

The proposed decentralized solution is used to implement the coordinated TD-ACOPF. In contrast, an isolated approach is also conducted in which the transmission grid and each distribution grid optimize the ACOPF based on a pre-defined boundary condition. Table I shows the total generation costs.

The total cost reductions of the coordinated approach in system #1 and system #2 are \$342 and \$2,325 respectively. Since only one time period is considered in the simulations, the above are hourly cost reductions and take 2.6% and 1.5% of the total generation costs of the two systems. It can be concluded that the coordination in ACOPF can provide a better balance of generation resources among transmission and distribution grids, and thus gives a lower total generation cost.

We further narrowed down the bus voltage limits in distribution grids from 0.9-1.1 (p.u.) to 0.94-1.06 (p.u.). In this case, the isolated approach fails to provide a feasible solution in System #2, whereas our proposed coordinated approach works well. This is because the pre-defined boundary voltage

TABLE I
GENERATION COSTS OF COORDINATED AND ISOLATED APPROACHES

		Coordinated Approach	Isolated Approach
System #1	Transmission	\$11,222	\$8,100
	Distribution	\$1,771	\$5,235
	Total	\$12,993	\$13,335
System #2	Transmission	\$145,435	\$151,219
	Distribution	\$5,253	\$1,794
	Total	\$150,688	\$153,013

TABLE II
GENERATION COSTS OF PROPOSED AND CENTRALIZED METHODS

		Proposed Method	Centralized Method
System #1	Transmission	\$11,222	\$11,222
	Distribution	\$1,771	\$1,771
	Total	\$12,993	\$12,993
System #2	Transmission	\$145,435	\$145,435
	Distribution	\$5,253	\$5,253
	Total	\$150,688	\$150,688

TABLE III
ROOT-MEAN-SQUARE ERRORS OF THE PROPOSED METHOD TO THE CENTRALIZED METHOD ON BOUNDARY VARIABLES

	Active Power	Reactive Power	Voltage Magnitude
System #1	6.8×10^{-5}	8.3×10^{-4}	2.2×10^{-6}
System #2	4.6×10^{-5}	6.0×10^{-3}	6.2×10^{-6}

magnitude is deemed unreasonable in the isolated approach, causing the failure of distributed generators to integrate. Thus, the proposed coordinated approach avoids overvoltage problems by coordinating transmission and distribution grids. The coordinated solutions can enhance the system operation by offering a proper reactive power and voltage control solutions in extreme scenarios.

C. Performance of the Proposed Method

1) Exactness: To examine whether the proposed decentralized method could provide an exact solution for the coordinated TD-ACOPF, we first compare the optimal generation costs of our proposed method and the centralized method. The results are shown in Table II where no error was found on our proposed method with respect to the total generation cost. In addition, the root-mean-square relative errors of the proposed method to the centralized method on the boundary transferred power and boundary bus voltage magnitude are computed in Table III.

In Table III, the errors are small enough and acceptable. The reactive power errors are relatively higher because the total generation cost is not quite sensitive to reactive power. However, the accuracy could be improved by setting a smaller convergence tolerance ε in (34).

Note that second-order cone relaxations were not applied in the centralized method because the centralized method used the entire grid to compute ACOPF. Consequently, the errors in Table III represent errors from both the proposed decentralized method and the second-order cone relaxation. From this perspective, the error introduced by the proposed decentralized error could be much smaller. This observation also proves that the second-order cone relaxation of the distribution grid ACOPF is almost exact.

TABLE IV
PERFORMANCE COMPARISON OF DIFFERENT DECENTRALIZED METHODS

	System #1		System #2	
	Iteration Number	Time (s)	Iteration Number	Time (s)
Proposed	5	0.95	14	9.12
GBD	20	3.63	Numerical Problems	
HGD	Converged to wrong result		Did Not Converge	
ADMM	Did Not Converge		Did Not Converge	
ALD	Did Not Converge		Did Not Converge	
APP	Did Not Converge		Did Not Converge	

2) Convergence Speed: The proposed decentralized method is compared with the generalized Benders decomposition (GBD), the heterogeneous decomposition (HGD) [9], the alternating direction method of multipliers (ADMM), the augmented Lagrangian decomposition (ALD), and the auxiliary problem principle decomposition (APP). The comparison terms include iteration numbers and computation times. The results for both systems are given in Table IV.

The proposed method provides a more scalable and robust solution as compared with other methods. The whole procedure of the proposed method took 0.95 and 9.12 seconds for the two systems respectively. The time consumption is acceptable, although higher than the isolated approach in Section IV-B which are 0.14 and 0.20 seconds. However, the proposed method provides a more economic result and avoids infeasible security issues.

In system #2 of the GBD method, sub-problems failed to get a feasible solution even with feasible cuts added because of numerical problems. In system #1 of the HGD method, it converges to another result which has a far worse total generation cost and might be a saddle point. Since the HGD method uses a fixed iteration algorithm based on the first-order optimality condition to decompose transmission and distribution grids, there is no guarantee that it converges properly. Because five controllable DGs are integrated in each distribution grid, the spectral radius of the fixed iteration for TD-ACOPF approaches 1.0, which leads HGD to diverge in system #2. In dual decomposition methods ADMM, ALD, and APP, we tried setting the dual multiplier updating step size as 0.001, 0.01, 0.1, 1, and 10, but none of the above settings converged within 500 iterations in both systems.

The comparison between the proposed method and the GBD method in System #1 also shows that although the computation complexity of the proposed method is higher during each iteration, its fast convergence could reduce the overall computation time.

The gaps between upper and lower bounds of the proposed method of both systems are plotted in Fig. 3 to provide a more intuitive view of the iteration procedure. Since infeasibility sub-problems might occur during the iteration of the GBD method, the gaps of GBD are not taken into comparison. It

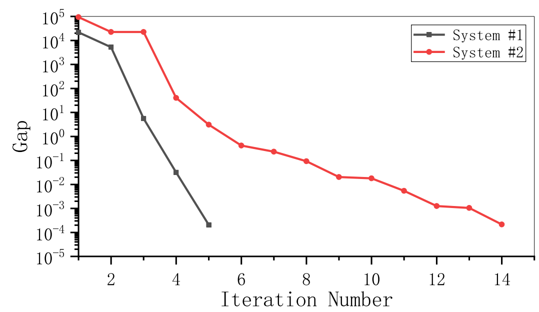

Fig. 3. Reduction in gap during iterations – proposed method.

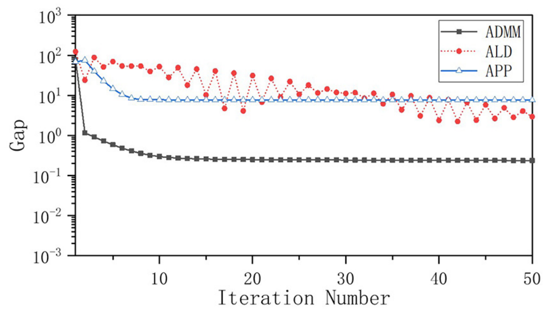

Fig. 4. Reduction in gap during iterations – dual decomposition methods.

can be seen that the gap decreasing speed of the proposed method is approximately exponential.

We further investigate the gaps of the dual decomposition methods, which are not converged in our case studies. Note that the gaps of dual decomposition methods are defined based on boundary variables, which are different from the gaps of our proposed method. Therefore, we don't compare the two different gaps in a single figure. Fig. 4 shows the gaps of the ADMM, ALD, and APP in system #1. The dual multiplier updating step size was set as 1 for ADMM and ALD, and 10 for APP.

It can be seen from Fig. 4 that the gaps of ADMM and APP stopped decreasing at a certain level, while the gap of ALD decreases as well as oscillates, but still far from the required termination criterion, which is 0.001. Hence, dual decomposition methods are not stable and robust enough for solving TD-ACOPF.

V. Conclusion

In this paper, a decentralized solution is proposed for the coordinated ACOPF of the integrated transmission and distribution grid. The proposed TD-ACOPF problem is characterized by a transmission grid OPF model in polar coordinates and a distribution grid branch flow model. A distribution-cost-correction framework is developed, and the second-order cone relaxation is applied on distribution grid models to guarantee the convergence. Based on this framework, a decentralized method is implemented by proposing lower bound functions and quadratically approximated functions of distribution grid costs. The proposed decentralized method has been tested on two case studies with different scales. The simulation results verify the advantages of the coordinated ACOPF as compared to those of the isolated approach with respect to operational economy and security. The results also demonstrate that the performance of the proposed method is accurate, computationally fast, robust, and more scalable than the traditional decentralized methods.

Appendix

In our proposed TD-ACOPF model, the transmission grid uses a nonconvex ACOPF model. Thus, it cannot be guaranteed that the solution achieved is globally optimal. However, for the ACOPF of most transmission grids, since the objective function is convex, the same locally optimal solution can be found through the interior-point method even if starting with different initial points. In other words, there exists a stable locally optimal solution for the nonconvex transmission grid ACOPF, and it is usually the global optimum. In the following discussions, it is assumed that stable locally optimal results can be achieved for the nonconvex transmission grid ACOPF.

A. Convergence of the Simple Implementation

We first prove that the simple implementation of the distribution-cost-correction framework (Section III-B) has finite convergence.

Proof: As the iteration number m increases, the number of constraints in (32c) is growing. Therefore, the $LB^{(m)}$ solved from problem (32) is increasing but will not be greater than the optimal generation cost of the entire transmission and distribution grid. We assume that the lower bound $LB^{(m)}$ converges to a point $\overline{LB}$ that has a gap to the optimal generation cost of the entire transmission and distribution grid. The optimal solution of (32) converges to $\overline{\mathbf{x}_T}$ and $\overline{\alpha_k}$. The lower bound functions generated by each distribution grid at $\overline{\mathbf{x}_T}$ is denoted as $\overline{L_{D_k}}(\mathbf{g}_k)$.

Since the lower bound function $\overline{L_{D_k}}(\mathbf{g}_k)$ is a tangent plane of the convex distribution cost function $C_{D_k-T}(\mathbf{g}_k)$ at $\mathbf{G}_k(\overline{\mathbf{x}_T})$, there are:

$$C_{D_k-T}(\mathbf{G}_k(\overline{\mathbf{x}_T})) = \overline{L_{D_k}}(\mathbf{G}_k(\overline{\mathbf{x}_T})) \quad (47)$$

and

$$C_{D_k-T}(\mathbf{G}_k(\mathbf{x}_T)) > \overline{L_{D_k}}(\mathbf{G}_k(\mathbf{x}_T)),\ \textit{for any}\ \mathbf{x}_T \neq \overline{\mathbf{x}_T} \quad (48)$$

Therefore, at $\overline{\mathbf{x}_T}$ and $\overline{\alpha_k}$, $\overline{\alpha_k}$ equals $\overline{L_{D_k}}(\mathbf{G}_k(\overline{\mathbf{x}_T}))$ and is greater than any other tangent planes generated at other points. We have:

$$\begin{aligned}\overline{LB} &= C_T(\overline{\mathbf{x}_T}) + \sum_{k\in ID} \overline{\alpha_k} \\ &= C_T(\overline{\mathbf{x}_T}) + \sum_{k\in ID} C_{D_k-T}(\mathbf{G}_k(\overline{\mathbf{x}_T}))\end{aligned} \quad (49)$$

We denote the actual optimal solution of the entire grid by a superscript * (e.g., for $\mathbf{x}_T$ is $\mathbf{x}_T^*$). There is:

$$\begin{aligned}&C_T(\overline{\mathbf{x}_T}) + \sum_{k\in ID} C_{D_k-T}(\mathbf{G}_k(\overline{\mathbf{x}_T})) \\ &\geq C_T\left(\mathbf{x}_T^*\right) + \sum_{k\in ID} C_{D_k-T}\left(\mathbf{G}_k\left(\mathbf{x}_T^*\right)\right)\end{aligned} \quad (50)$$

Let α_k^* be the maximum of all lower bound functions at $\mathbf{x}_T^*$. It is obvious that α_k^* is no greater than $C_{D_k-T}\big(\mathbf{G}_k\big(\mathbf{x}_T^*\big)\big)$ because each lower bound function is no greater than the actual cost function. Consequently,

$$\begin{aligned} \overline{LB} &\geq C_T\big(\mathbf{x}_T^*\big) + \sum_{k\in ID} C_{D_k-T}\big(\mathbf{G}_k\big(\mathbf{x}_T^*\big)\big) \\ &\geq C_T\big(\mathbf{x}_T^*\big) + \sum_{k\in ID} \alpha_k^* \end{aligned} \tag{51}$$

The result in (51) suggests that $\mathbf{x}_T^*$ and α_k^* is a more optimal solution than $\overline{\mathbf{x}_T}$ and $\overline{\alpha_k}$ for (32). This contradicts the supposition that the optimal solution of (32) converges to $\overline{\mathbf{x}_T}$ and $\overline{\alpha_k}$. Therefore, the simple implementation has finite convergence. ■

B. Convergence of the Revised Implementation

As we have added quadratically approximated functions $Q_{D_k}^{(m)}(\mathbf{g}_k)$ to problem (46), we then prove that the quadratically approximated functions will not break the convergence of the previous simple implementation.

Proof: Considering that the generations of upper bound $UB^{(m)}$ and lower bound $LB^{(m)}$ as well as the termination criterion remain unchanged, the only thing that needs to be proved is the introduction of constraint (46d) will not change the solution of (32) at its converged point $\mathbf{x}_T^*$ and α_k^*.

Since the quadratically approximated function is considered as an additional constraint in (46d), the optimality at the optimum of the entire grid ($\mathbf{x}_T^*$ and α_k^*) will not be affected by introducing (46d) as long as constraint (46d) is not active at $\mathbf{x}_T^*$ and α_k^*. It can be found that $Q_{D_k}^*(\mathbf{G}_k(\mathbf{x}_T^*))$ is equal to $C_{D_k-T}(\mathbf{G}_k(\mathbf{x}_T^*))$ because $Q_{D_k}^*(\mathbf{G}_k(\mathbf{x}_T^*))$ is deduced at the base point $\mathbf{G}_k(\mathbf{x}_T^*)$. Therefore, the condition that constraint (46d) is inactive at $\mathbf{x}_T^*$ and α_k^* holds. The convergence condition remains unchanged after the quadratically approximated function is introduced. ■

REFERENCES

[1] C. D'Adamo, S. Jupe, and C. Abbey, "Global survey on planning and operation of active distribution networks—Update of CIGRE C6.11 working group activities," in *Proc. 20th Int. Conf. Exhibit. Electricity Distrib. (CIRED)*, Prague, Czech Republic, 2009, pp. 1–4.

[2] V. F. Martins and C. L. T. Borges, "Active distribution network integrated planning incorporating distributed generation and load response uncertainties," *IEEE Trans. Power Syst.*, vol. 26, no. 4, pp. 2164–2172, Nov. 2011.

[3] S. Chowdhury, S. P. Chowdhury, and P. Crossley, *Microgrids and Active Distribution Networks*. London, U.K.: Inst. Eng. Technol., 2009.

[4] J. F. Benders, "Partitioning procedures for solving mixed-variables programming problems," *Numerische Mathematik*, vol. 4, no. 1, pp. 238–252, Dec. 1962.

[5] H. Gerard, E. I. R. Puente, and D. Six, "Coordination between transmission and distribution system operators in the electricity sector: A conceptual framework," *Utilities Policy*, vol. 50, pp. 40–48, Feb. 2018.

[6] Z. Li, Q. Guo, H. Sun, and J. Wang, "Coordinated economic dispatch of coupled transmission and distribution systems using heterogeneous decomposition," *IEEE Trans. Power Syst.*, vol. 31, no. 6, pp. 4817–4830, Nov. 2016.

[7] C. Lin, W. Wu, X. Chen, and W. Zheng, "Decentralized dynamic economic dispatch for integrated transmission and active distribution networks using multi-parametric programming," *IEEE Trans. Smart Grid*, vol. 9, no. 5, pp. 4983–4993, Sep. 2018.

[8] A. Khodaei and M. Shahidehpour, "Microgrid-based co-optimization of generation and transmission planning in power systems," *IEEE Trans. Power Syst.*, vol. 28, no. 2, pp. 1582–1590, May 2013.

[9] Z. Li, Q. Guo, H. Sun, and J. Wang, "Coordinated transmission and distribution AC optimal power flow," *IEEE Trans. Smart Grid*, vol. 9, no. 2, pp. 1228–1240, Mar. 2018.

[10] C. Lin, W. Wu, B. Zhang, B. Wang, W. Zheng, and Z. Li, "Decentralized reactive power optimization method for transmission and distribution networks accommodating large-scale DG integration," *IEEE Trans. Sustain. Energy*, vol. 8, no. 1, pp. 363–373, Jan. 2017.

[11] S. Boyd, N. Parikh, E. Chu, B. Peleato, and J. Eckstein, "Distributed optimization and statistical learning via the alternating direction method of multipliers," *Found. Trends® Mach. Learn.*, vol. 3, no. 1, pp. 1–122, Jan. 2011.

[12] S. J. Wang, S. M. Shahidehpour, D. S. Kirschen, S. Mokhtari, and G. D. Irisarri, "Short-term generation scheduling with transmission and environmental constraints using an augmented Lagrangian relaxation," *IEEE Trans. Power Syst.*, vol. 10, no. 3, pp. 1294–1301, Aug. 1995.

[13] A. J. Conejo, E. Castillo, R. Minguez, and R. Garcia-Bertrand, *Decomposition Techniques in Mathematical Programming*. New York, NY, USA: Springer, 2006.

[14] A. M. Geoffrion, "Generalized benders decomposition," *J. Optim. Theory Appl.*, vol. 10, no. 4, pp. 237–260, 1972.

[15] M. E. Baran and F. F. Wu, "Optimal capacitor placement on radial distribution systems," *IEEE Trans. Power Del.*, vol. 4, no. 1, pp. 725–734, Jan. 1989.

[16] M. Farivar and S. H. Low, "Branch flow model: Relaxations and Convexification—Part I," *IEEE Trans. Power Syst.*, vol. 28, no. 3, pp. 2554–2564, Aug. 2013.

[17] M. Farivar and S. H. Low, "Branch flow model: Relaxations and convexification—Part II," *IEEE Trans. Power Syst.*, vol. 28, no. 3, pp. 2565–2572, Aug. 2013.

[18] N. Li, L. Chen, and S. H. Low, "Exact convex relaxation of OPF for radial networks using branch flow model," in *Proc. IEEE 3rd Int. Conf. Smart Grid Commun. (SmartGridComm)*, 2012, pp. 7–12.

[19] (2019). *System Data for TD-ACOPF*. [Online]. Available: https://drive.google.com/file/d/1h97MdY7Uwp05wu29k5WkmI9Klq2JooWd/view?usp=sharing

[20] A. Wächter and L. T. Biegler, "On the implementation of an interior-point filter line-search algorithm for large-scale nonlinear programming," *Math. Program. A*, vol. 106, no. 1, pp. 25–57, 2006.

[21] R. D. Zimmerman, C. E. Murillo-Sánchez, and R. J. Thomas, "MATPOWER: Steady-state operations, planning, and analysis tools for power systems research and education," *IEEE Trans. Power Syst.*, vol. 26, no. 1, pp. 12–19, Feb. 2011.

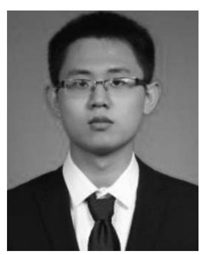

Chenhui Lin (S'16) received the B.S. degree in electrical engineering from Tsinghua University, Beijing, China, in 2015, where he is currently pursuing the Ph.D. degree with the Department of Electrical Engineering.

He was a visiting Ph.D. student with the Illinois Institute of Technology, Chicago, IL, USA, in 2019. His research interests focus on the operation and control of power system integrated with renewable energy.

Wenchuan Wu (SM'14) received the B.S., M.S., and Ph.D. degrees from the Department of Electrical Engineering, Tsinghua University, Beijing, China.

He is currently a Professor with the Department of Electrical Engineering, Tsinghua University. His research interests include energy management system, active distribution system operation and control, and machine learning and its application in energy system. He is currently an IET Fellow, and an Associate Editor of *IET Generation, Transmission and Distribution* and *IET Energy Systems Integration*.

Mohammad Shahidehpour (F'01) received the Honorary Doctorate degree from the Polytechnic University of Bucharest, Bucharest, Romania. He is a University Distinguished Professor, and a Bodine Chair Professor and the Director of the Robert W. Galvin Center for Electricity Innovation, Illinois Institute of Technology. He is a member of the U.S. National Academy of Engineering and fellow of the American Association for the Advancement of Science, and the National Academy of Inventors.